ISBN: 978-3-95450-233-2 ISSN: 2673-5504 doi:10.18429/JACoW-SRF2021-MOPTEV009

A METHOD FOR IN-SITU Q0 MEASUREMENTS OF HIGH-QUALITY SRF RESONATORS*

Sergey Kuzikov†[1], Pavel Avrakhov[1], Chunguang Jing[1], Roman Kostin[1], Yubin Zhao[1]
Euclid Techlabs LLC, Bolingbrook, IL, USA
[1]also at Euclid Beamlabs LLC, Bolingbrook, IL, USA
Tom Powers, Robert Rimmer, JLab, Newport News, Virginia, USA
Vyacheslav Yakovlev, FNAL, Batavia, Illinois, USA

Abstract

Accelerator projects such as LCLS-II naturally require low-loss superconducting (SRF) cavities. Due to strong demand for improving intrinsic quality factor (Q0), importance of accurate cavity characterization increases. We propose a method to measure Q0 in situ for an SRF resonator installed in its cryogenic module and connected with a RF feed source via a fixed RF coupler. The method exploits measurements of a response for an SRF resonator fed by an amplitude-modulated signal. Such a signal can be synthesized as a beat-wave composed of two frequencies that are close to the resonant frequency. Analyzing the envelope of the reflected signal, one can find the difference in reflection for the chosen frequencies and use them to compute the intrinsic Q. We also develop the methodology to carry out measurements of Q0 at the nominal cavity operating voltage. We verified our method in experiments with a room temperature copper resonator and with two SRF resonators including Fermilab's 650 MHz cavity and JLab's 1500 MHz cavity.

INTRODUCTION

Although SRF resonators have extremely high Q-factors (10^6–10^7 loaded quality factor, and 10^{10}–10^{11} unloaded quality factor, Q0) there are well-developed methods to measure these values. However, problems arise when an SRF resonator installed in a cryogenic module is connected to a feeding RF source via a fixed RF coupler. In this case, there are no direct ways to measure the degradation of Q_0 in situ. Measurement of the cryogenic heat load is the only method that can be used in this case. However, when several cavities are housed in a common cryomodule, measuring individual Q_0 values can be time consuming, since each cavity needs to be operated individually in order to identify the heat load increase produced by that particular cavity. The method proposed in this paper circumvents this drawback by offering a direct and faster measurement for each individual cavity. We also propose a methodology to carry out the measurements of Q_0 at high accelerating voltages, or even at the nominal cavity operating voltage. These measurements are most beneficial, because Q_0 at the nominal accelerating voltage can differ considerably from the low-field value of Q_0. Therefore, there is a particular need for accurate and fast in situ Q-factor measurements. The procedure should not require removing the RF coupler, which introduces additional loss that interferes with the direct measurements.

We suggest the generation of a beat wave, which introduces the superposition of two frequencies. One frequency is to be tuned exactly to the test cavity resonance, and the second shifted off of the resonance. The beat wave provides information on the difference in reflection (or transmission) on resonance and off resonance. In case of the reflected beat-wave measurements, this difference is inversely proportional to the intrinsic Q-factor and can be used to retrieve it. In the case of transmitted signal measurements at a pick-up, the mentioned difference depends on Q_0 in a more complicated form, but still can be used to retrieve Q_0.

A CONCEPT FOR Q0 MEASUREMENTS

The reflection of a monochromatic signal from a resonator having high beta factor ($\beta=Q_0/Q_{ext}$ – ratio of intrinsic and external Q-factors) is very close to unity. That is why direct measurement of the resonant reflection curve of such cavities requires the use of modern network analyzers with a very large dynamic range [1]. The loaded Q-factor is frequently measured as the inverse decay time of the stored energy in a radiating resonator that has been previously energize at the resonant frequency [2].

The measurement procedure can be simplified if one makes use of a reference signal, so that the reflected signal can be measured relative to the reference signal (Fig. 1a). Reformulating the problem, in this case it is only the difference between these two signals that needs to be measured (Fig. 1b). Let us consider the superposition of two frequency components, f_0 and $f_0+\Delta f$, with equal amplitudes and closely spaced frequencies (Fig. 1a). The mentioned superposition of the two frequencies is the beat-wave signal, where the beat frequency corresponds to the frequency difference between these two components. Each frequency component will be reflected from the high-Q resonator with close to unity reflection (Fig. 2a), but with slightly different amplitudes and essentially different phases (Fig. 2b). Using a broadband oscilloscope, one can measure the beat wave with high accuracy. Assuming that the amplitudes of the components of the incident beat wave were selected to be equal to each other, the minimum of the incident wave envelope will be exactly zero. For the reflected beat wave, the minimum will become greater than zero, and the greater the difference in the reflection coefficients for the selected test frequencies, the greater the value of the

---

* This work was supported by DoE SBIR grant # DE-SC0019687.
† s.kuzikov@euclidtechlabs.com

measured minimum will be. The difference Δ*R* can be measured and can be used to calculate Q_0 in accorda2nce with the known formula:

$$Q_0 = \frac{2Q_l}{1-R(f_0)} \approx \frac{2Q_l}{R(f_0+\Delta f)-R(f_0)} \quad (1)$$

where Q_l – is a loaded Q-factor. The loaded Q factor, which one needs to know to evaluate equation (1), could be measured according to [3] or using the beat-wave technique via the group delay for the beat-wave envelope.

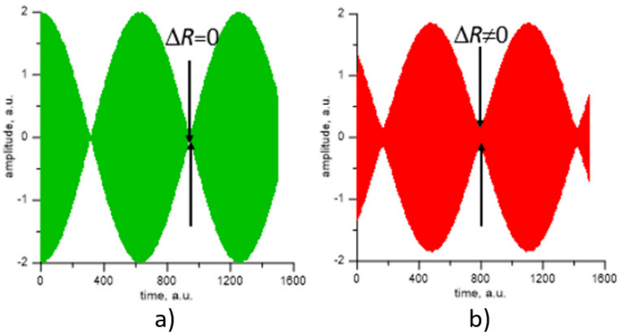

Figure 1: Incident beat wave with equal amplitudes of frequency components (a) and beat wave reflected from SRF cavity (b), where zeros are lost due to the difference in reflection for resonant and off-resonant frequencies.

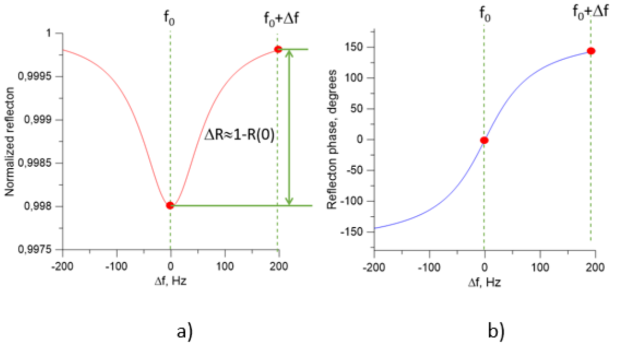

Figure 2: Amplitude of reflection for resonator with $Q_0=1\times10^{10}$ and $Q_l=1\times10^{7}$ vs frequency shift from resonant frequency f_0=650 MHz (a) and phase of reflection for the 650 MHz resonator (b).

Analysis of Method Uncertainties

In order to explore the capabilities of the method, it was first necessary to solve a problem that arises when an ideal resonator is replaced by a realistic resonator. In the realistic case, an SRF resonator has a physically long coupler, which inevitably brings some its own reflections and additional signal attenuation. The realistic resonator could be represented in the form of the scheme shown in Fig. 3, where the entire system consists of the chain: spurious reflector – transmission line with some losses – test (ideal) resonator. The reflection from this system depends on the spurious reflection amplitude, phase, and line length. We analyzed reflection characteristics of the realistic resonator. In Fig. 4 one can see reflection plots for different phases (transmission line lengths), where the spurious reflection was as large as -35 dB, losses in the line were as large as 0.6% (correspond to estimates done for Fermilab's conduction-cooled 650 MHz resonator [4]. The numerical analysis has shown that for the considered case the actual spread of Q_0 measurement would be satisfactory, as large as 30%. The larger the spurious reflection and losses, the bigger the Q_0 errors will be.

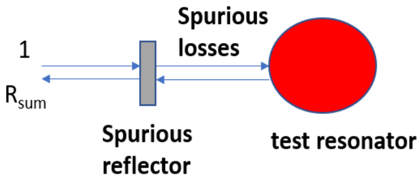

Figure 3: Realistic resonator consisted of test resonator and spurious reflector connected to transmission line with losses.

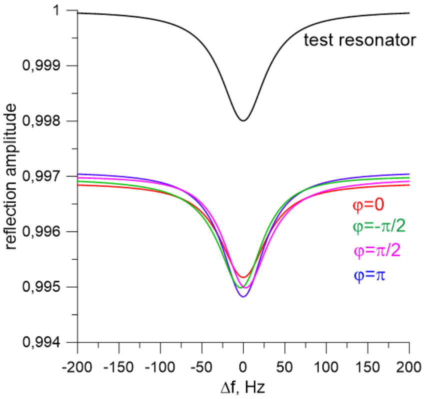

Figure 4: Reflection from 650-MHz SRF resonator ($Q_0=1\times10^{10}$ and $Q_l=1\times10^{7}$) accompanied with -35 dB spurious reflection and 0.6% power loss in the transmission line.

Let us consider a measurement scheme and calibration procedure to set up equal amplitudes of the two frequency components in the beat wave. The typical scheme for measurements at low-power level may look like Fig. 5. Here, in the normal regime, a high-power amplifier feeds an accelerating resonator. If necessary, the high-power amplifier can be turned off, and then the low-power, highly stabilized, two-frequency RF source would feed the structure. The calibration procedure should be set up as follows. To use a directional coupler as close as possible to the test resonator and a broadband oscilloscope, in order to register the reflected beat wave. Next step is to turn the SRF resonator on and to set the first frequency at resonance using a pick-up probe installed at the resonator. This frequency has to be locked to the resonator frequency (to avoid errors due to microphonics). The second frequency is not seen by this probe. Varying amplitudes of the frequency components, one should establish the zeros in the beat wave. In the previous step, we obtained equal amplitudes of the two frequency components, but in the reflected beat wave from the SRF resonator. That is why, in the last step, we have to turn the resonator off. This could be done either by substituting a short for the resonator or by detuning the resonator by means of a tuner, in order to shift both frequencies far up or down from the resonance.

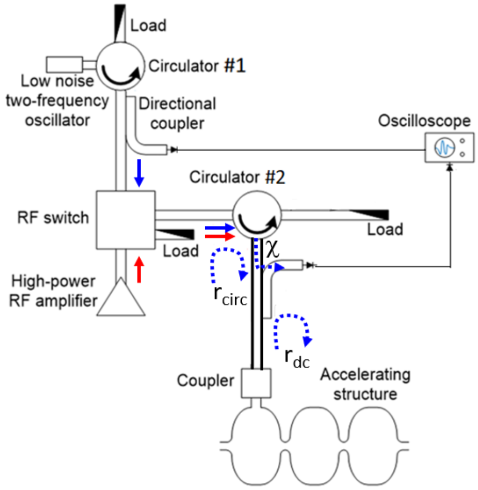

Figure 5: Scheme for low-power measurements showing first-order RF signal contamination.

Study of RF Signal Contaminations and Accuracy Improvement

The next step of the analysis method is to study unavoidable RF signal contamination caused by non-ideal RF components (circulators, directional couplers, dummy loads, RF switch) located outside of the cryomodule. These contaminating signals cause some change in the signal received by the directional coupler. Actually, the reflected signal could be represented as a sum of the test resonator reflection R_{res} plus the contaminating signal, i.e. $R=R_{res}+R_{con}$. First of all, all contaminating signals can be classified in accordance with a perturbation theory. Assuming that all the RF components are almost ideal, we can neglect the multiple reflections of RF signals from different components, because contribution of such high-order contaminating signals should be small. That is why we chose to consider only the first-order contaminating signals, which are the largest and most deleterious. In particular, first-order RF contamination can be caused by the signal from the receiving directional coupler not being reflected at all from the test resonator, due to the finite directivity of the receiving coupler. The RF radiation path for this case is shown by the dashed arrow with the caption "χ" in Fig. 6. Mathematically, the full received signal in this case can be represented as $R(f)=R_{res}(f)+\chi\times\exp(i\varphi)$, where χ - is a coefficient of the directivity and φ - is the relative phase between the test resonator signal and the contaminating signal.

Other first-order contaminations could be born due to reflection of the signal traveling to the SRF resonator from the circulator or from the directional coupler (see Fig. 5, where the mentioned contaminating signals are shown by dashed arrows with captions "r_{circ}" and "r_{dc}" correspondingly). In this case, the full received RF signal can be written as $R(f)=R_{res}(f)\times(1+R_{res}(f)\times\xi\times\exp(i\varphi))$, where $\xi=r_{circ}$ or $\xi=r_{dc}$. Because, in our case, $|R_{res}(f)|\approx 1$, this case is similar to the previously considered case. The previously considered 650 MHz resonator ($Q_0=1\times10^{10}$, $\beta=10^3$) was simulated. The Fig. 6 shows that the high coupler directivity (-70 dB) provides good Q_0 accuracy for arbitrary mutual phase φ (the measured Q_0 is less than 50% different from the exact value). In the case of -40 dB directivity, the results are satisfactory for some phases, but for other phases the errors exceed ten times. The reason is that the phase of reflection from the test cavity sharply depends on frequency (Fig. 2b). The phase difference at the resonance frequency and far from resonance reaches π. In contrast, the phase of the contaminating signal does not depend on frequency in the considered narrow frequency band.

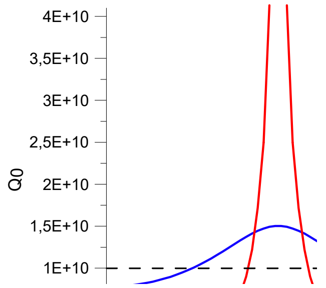

Figure 6: Simulation of Q_0 measurements versus the phase of the contaminating signal for two values of coupler directivity:-40 dB (red) and -70 dB (blue), respectively.

The described results encouraged us to invent an improved method for the Q_0 retrieval procedure. The idea is that one needs to phase the test resonator signal correctly with respect to the contaminating signal to allow us to work with in-phase signals. In the Fig. 6, the in-phase condition corresponds to the phase 0 (or 2π). At this phase, the full resonant curve becomes wider and deeper in comparison with the original test resonator curve. The deeper curve leads to a systematic decrease of the Q_0 calculated by equation (1). This Q_0 decrease is caused by the contaminating signal. Therefore, one can take it into account using a modified (corrected) equation for the Q_0 calculation:

$$Q_0 = \frac{2Q_l}{R(f_0+\Delta f)-R(f_0)-2\chi} \qquad (2)$$

In order to use this equation, one needs to measure the contaminating signal χ. We propose to carry out the measurement of the undesirable contaminating signal by means of phase shifters. The resonator must be detuned for this measurement. Varying the phase, one should determine the full signal minimum R_{min} and maximum R_{max} at the receiving directional coupler. The average of these values allows one to obtain the magnitude of the contaminating signal necessary to evaluate equation (2) as $\chi=(R_{max}-R_{min})/2$. The next steps must be to substitute sections of a regular waveguide (or coaxial cable) of the proper length that corresponds to the insertion phase of the phase shifter that provided the signal maximum. Second, one needs to tune the test cavity to the resonance and to measure $R(0)-R(\Delta f)$ using the beat-wave technique and determine the decreased (in comparison with the correct) Q_0 value and then to calculate the adjusted Q_0 value using equation (2). Note that it is necessary to perform the measurement of the contaminating signal only once at the beginning of resonator operation.

The Fig. 7 shows how good Q_0 accuracy can be achieved if the corrected procedure based on equation (2) is used. Again, for these simulations, we made use of the 650 MHz resonator.

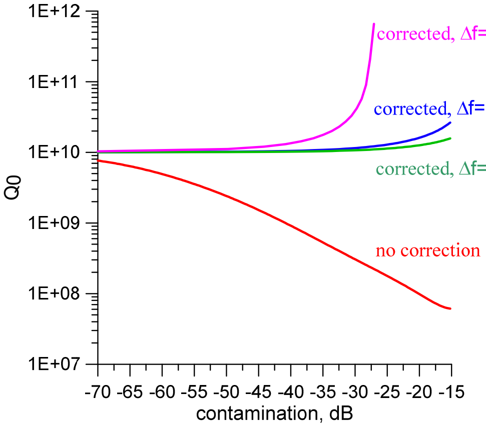

Figure 7: Simulation of Q_0 measurement in the advanced mode.

EXPERIMENTAL DEVELOPMENT OF MEASUREMENT TECHNIQUE

Measurement of Q-Factor for a Room Temperature Test Resonator

The purpose for this experiment was to test calibration procedure and RF box which has to generate two frequencies. For measurements at room temperature, we employed a 1.3-GHz copper resonator that was previously used in AWA for particle acceleration (Fig. 8).

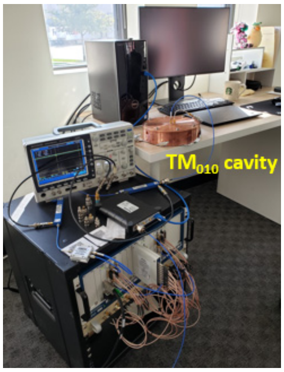

Figure 8: 1.3 GHz room temperature copper resonator.

This resonator had 7×10^3 loaded quality factor with β~1. In order to increase the coupling factor, we redesigned the resonator's coupler. As a result, the coupling factor was increased by almost two orders of magnitude and the loaded quality factor was reduced to 70–100. The intrinsic Q_0 was estimated as 5×10^3. The two-frequency RF radiation was generated by means of the fabricated RF electronic equipment, but, of course, frequency locking was not necessary, since microphonics were absent. In the final stage of tests, we recorded the incident as well as reflected beat waves by means of an 8 GHz LeCroy oscilloscope (Fig. 9). The frequency shifts between the beat-wave components were as large as 20 MHz. The recorded data allowed the calculation of the loaded Q-factor as well the intrinsic Q-factor. The loaded Q was in excellent agreement with the true value. The intrinsic Q-factor calculation results were very close to the true value (Q_0=4500).

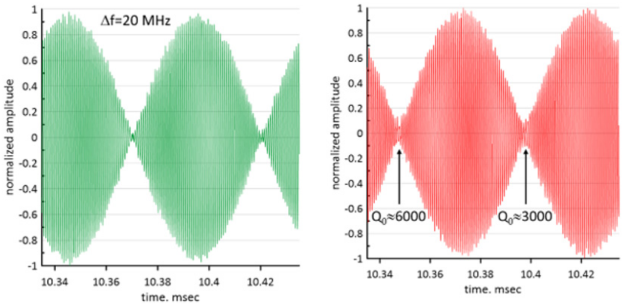

a) b)

Figure 9: Resonator response: a - calibration signal (resonator is turned off), b – reflected signal when resonator is turned on.

Q_0 Measurements of 650-MHz SRF Cavity in Presence of Microphonics

For the 650-MHz SRF resonator at Fermilab, microphonics substantially exceeded 10 Hz. The resonator was conduction-cooled (Fig. 10). The resonator was designed for β≈1 with $Q_l=6\times10^9$– 9×10^9. It was not possible to change the mentioned coupling factor, because that might require the installation of a new coupler. That is why, we used a three-stub tuner in the feeding antenna to increase slightly the coupling.

Figure 10: Set up of the conduction-cooled 650-MHz SRF resonator in Fermilab.

The Q-measurement tests were carried out in the regimes where the frequency shift of the beat-wave components was 100 kHz, 10 kHz, and 10 Hz. In the Fig. 11 the shift was as large as 100 kHz. The equipment worked to lock the first frequency of the beat wave to the lowest on-frequency resonance using the resonator pick-up's signal. We installed a 12-GHz Tektronix oscilloscope to record the beat-wave oscillograms. The sample rate was as high as 6.25 GS/s. Remarkably, in all cases, frequency locking allowed one to reliably record the beat waves. The stability was pretty high. The Q_0 value, which could be calculated from experimental data, was as high as $Q_0 \approx 2 \cdot 10^{10}$ ($\beta \approx 3$). In this test we showed that the elaborated electronics can work in presence of strong microphonics.

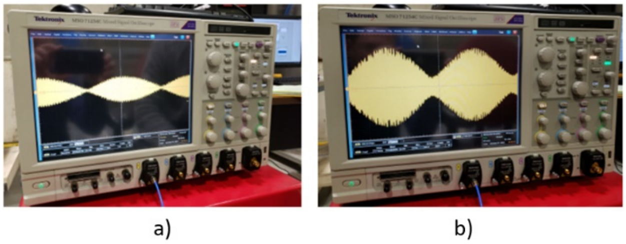

Figure 11: Calibrated beat wave when resonator is turned on (Δf=100 kHz) (a), reflected signal from the short (Δf=100 kHz) (b).

Q_0 Measurements of Higher-Beta 1500-MHz SRF Cavity at JLab

Experiments at JLab were carried out with a CEBAF 1500 MHz SRF resonator whose loaded Q factor was as high as $Q_l = 6.6 \times 10^6$ [5]. The goal of this experiment was to explore contamination influence on the high-beta ($\beta \approx 360$) SRF resonator. In this experiment, for measurement reasons, the RF signals were down converted to 5 MHz. In this case, the data came out really nice, and we could easily see where things were zeroing out.

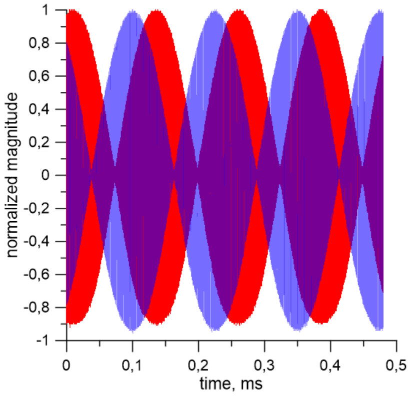

Figure 12: Oscillograms of signals (Δf=8 kHz): a – calibrated signal (blue) and reflected signal (red).

The Fig. 12 shows the results of beat-wave records (for Δf=8 kHz). The zoom picture near beat wave minimum is shown in the Fig. 13. The calibrated beat wave (blue curve) was recorded when the resonator was turned on, when a short reflected all RF power the red curve was recorded which was used for Q_0 retrieve. The measured Q_0 did not exceed $5 \cdot 10^8$, but the true value was as high as $Q_0 = 2.4 \cdot 10^9$ (in accordance with [5]). This allows to conclude that contaminations were large enough so that high accuracy of Q_0 for strongly overcoupled ($\beta \sim 10^3$) resonators could be obtained using the proposed phasing technique only which allows to increase accuracy in presence of contaminated signals.

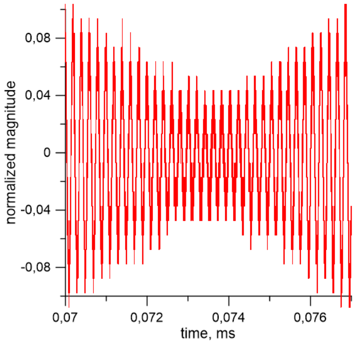

Figure 13: Zoom of the analysed signal.

Measurements at High Power Level

The scheme of measurements at high power levels is shown in Fig. 14. Here, a high-power klystron works in a nominal regime powering an empty (without beam) resonator. Here, we measure a beat wave composed at a pick-up. The beat wave in this case is a superposition of the transmitted klystron's power at frequency f_0 and a low power reflected signal at the shifted frequency $f_0 + \Delta f$.

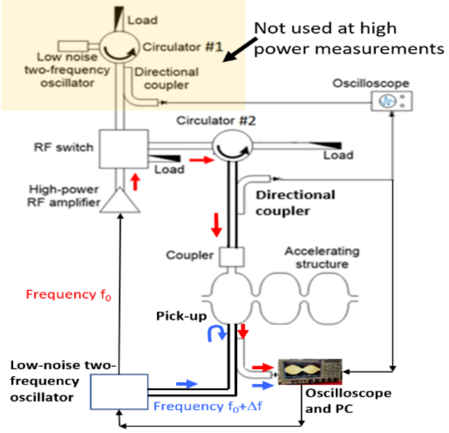

Figure 14: Scheme of a setup for Q_0 measurements at high-power level.

REFERENCES

[1] T. Powers, "Theory and Practice of Cavity RF Test Systems," 12th International Workshop On RF Superconductivity, 10-15 Jul 2005, Ithaca, New York. `https://www.osti.gov/biblio/890534`

[2] M. Liepe *et al.*, "Pushing the Limits: RF Field Control at High Loaded Q," in *Proc. of the Particle Accelerator Conference (PAC'05)*, 2005. `doi:10.1109/PAC.2005.1591213`

[3] Frank Marhauser, "Method for in situ and in operando cavity loaded Q extraction in superconducting rf accelerators", *Phys. Rev. Accel. and Beams,* vol. 24, p. 032001, 2021. `doi:10.1103/PhysRevAccelBeams.24.032001`

[4] J. P. Holzbauer *et al.*, "Systematic uncertainties in RF-based measurement of superconducting cavity quality factors," *Nuclear Instruments and Methods in Physics Research Section A*, vol. 830, no. 11, pp.22–29. `doi:10.1016/j.nima.2016.05.025`

[5] Charles E. Reece, "Continuous wave superconducting radio frequency electron linac for nuclear physics research", *Phys. Rev. Accel. and Beams,* vol. 19, p. 124801, 2016. `doi:10.1103/PhysRevAccelBeams.19.124801`